TRANSACTIONS OF THE INSTITUTE OF FLUID-FLOW MACHINERY

No. 139, 2018, 23–44

J. Grzelak* and Z. Wierciński

Experimental analysis of the freestream length scale and turbulence intensity impact on bypass transition in boundary layer on a flat plate

Institute of Fluid Flow Machinery Polish Academy of Sciences, Fiszera 14, 80-231 Gdańsk, Poland

Abstract

An experimental investigation of the turbulent flow over a flat plate in a subsonic wind tunnel was carried out. The enhanced level of turbulence was generated by five wicker grids with square meshes, and different parameters (diameter of the grid rod 0.3–3 mm and the grid mesh size 1–30 mm). The velocity of the flow was measured by means of a 1D hot-wire probe, suitable for measurements in a boundary layer. The aim of the investigation was to explore the turbulence length scale in the flow behind grids and to study its influence on the onset of laminar-turbulent bypass transition in a boundary layer on a flat plate. To assess the isotropy of turbulence, the skewness and kurtosis factors of the flow velocity distribution were determined. Several longitudinal scales of turbulence were determined and compared (integral, dissipation, Taylor microscale, and Kolmogorov scale) for different grids and different velocities of the mean flow 4, 6, 10, 15, and 20 m/s.

Keywords: Turbulence scale; Boundary layer; Bypass transition; Grid; Isotropic turbulence

*Corresponding author. E-mail adress: jj@imp.gda.pl

Nomenclature

$\bar{A}$	–	average, $\frac{1}{n}\sum_{(i=1)}^{n} A_i$
$\langle A \rangle$	–	time average
a	–	acceleration parameter
C_k	–	Kolmogorov constant
C_ε	–	constant in Eq. (14)
d	–	diameter of a grid rod
$D(k)$	–	dissipation spectrum
$E(k)$	–	turbulence energy spectrum
i	–	plate angle of attack
k	–	longitudinal wave number, coefficient of the formula (21)
k_d	–	wave number corresponding to l_d scale
k_e	–	wave number corresponding to l_e scale
k_η	–	wave number corresponding to the Kolmogorov scale
K_T	–	turbulent kinetic energy
$K(u)$	–	kurtosis factor
L	–	integral length scale
l	–	turbulence length scale
l_d	–	scale of the eddies corresponding to the maximum of dissipation spectrum
l_e	–	scale of the eddies corresponding to the maximum of energy spectrum
L_S	–	distance between the grid and the leading edge of the plate
Lu	–	dissipation length scale
M	–	mesh size
m	–	exponent of the formula (21)
r	–	radius of the plate leading edge
$R(\tau)$	–	time correlation coefficient
Re_x	–	Reynolds number
$\mathrm{Re}**$	–	momentum thickness Reynolds number
Re_λ	–	Taylor Reynolds number
$S(u)$	–	skewness factor
t	–	time
Tu	–	turbulence scale
U	–	velocity in x direction
x	–	streamwise distance

Greek symbols

$\delta**$	–	momentum thickness
ε	–	rate of dissipation of turbulence kinetic energy
η	–	Kolmogorov length scale
λ	–	Taylor length microscale
τ	–	time increment
τ_E	–	turbulence time microscale
ν	–	kinematic viscosity

1 Introduction

The external turbulence causes an earlier by-pass laminar, turbulent transition of the flow in a boundary layer which consequently leads to an increase of skin friction. It is possible to characterize the turbulence by its two main measures: intensity (usually related to a velocity along an average stream line) and scale (which has a linear dimension in case of length scale). The influence of turbulence intensity on transition is quite well known. The formulas describing the relation between the intensity and the onset Reynolds number are given for example by Mayle [1], Hall and Gibbings [2] or Abu-Ghannam and Shaw [3]. But there are still very few investigations relating to the influence of the turbulence scale on laminar-turbulent transition. Mayle, in his review, suggested that the transition appears earlier when the mesh of the grid is smaller (what implies a smaller length scale) [1]. Also Jonas, Mazur, and Uruba suggested that the inception and the transition length depend on the turbulence scale [4]. The authors of both papers claim that the use of their correlations are rather limited. Experimental results of [4] indicate that the boundary layer laminar-turbulent inception moves downstream with the decreasing of turbulence scale; the length of transition also becomes shorter. For larger values of dissipation length scale, Lu, the laminar-turbulent transition process ends earlier. The turbulence intensity at the leading edge of the plate was maintained constant ($Tu = 3\%$), whilst the values of the dissipation length scale were changing: ($2.2 < Lu < 33.3$) mm. The outcome of the investigation was a following correlation:

$$\mathrm{Re}_t^{**} = (245/Lu)^{0.535} \,, \tag{1}$$

where $\mathrm{Re}_t{}^{**}$ is the momentum thickness Reynolds number, $\mathrm{Re}_t^{**} = U\delta_t^{**}/\nu$, at the onset of transition, here U is the mean flow velocity, $\delta_t{}^{**}$ is the momentum thickness at the onset of transition, and ν is the kinematic viscosity of the fluid. Definitions of turbulence intensity and scales are precisely described below. Unfortunately, the above correlation is not dimensionless (the scale of turbulence has of course the dimension of length).

In the other author's opinion (e.g., [5]) it seems to be quite opposite to the results of investigations presented in [4]: the reducing of turbulence scale should provide an earlier inception, i.e., at the lower momentum thickness Reynolds number. That is why the previous investigations require some revision.

2 Review of turbulence scales definitions

Barrett and Hollingsworth describe few longitudinal scales of turbulence, although the authors report there are more than ten [6]. One can distinguish the integral scales – which are associated with the largest eddies in the flow, dissipation scales, microscales and Kolmogorov scales. The longitudinal integral scale can be defined as follows:

$$L = U \int_0^\infty \mathbf{R}(\tau)\, d\tau \ , \tag{2}$$

where $T_E = \int_0^\infty \mathbf{R}(\tau)\, d\tau$ is called *the Eulerian integral time scale* [7] and $\mathbf{R}(\tau)$ is a time correlation coefficient:

$$R_{ii}(\tau) = \frac{\langle u_i(x,t)\, u_i(x,t+\tau)\rangle}{\sqrt{\langle u_i^2(x,t)\rangle \ \langle u_i^2(x,t+\tau)\rangle}} \ . \tag{3}$$

The velocity field is described by the coordinate system ($i = x, y, z$) where x is an axis oriented in the direction of the mean flow velocity ($U = U_x, U_y = U_z = 0$). Velocity U and its fluctuations u describe variables in the x direction, U_y and u_y in the y direction, U_z and u_z in the z direction. In case of the isotropic turbulence the turbulence characteristics do not depend on the spatial orientation of the coordinate system ($\overline{u^2} = \overline{u_y^2} = \overline{u_z^2}$) [7].

Another length scale is related to the dissipation of turbulent kinetic energy. It can be interpreted as an average dimension of the eddies containing most of the energy (so-called 'energy scales') [6]. Assuming that the turbulence is isotropic, and knowing that the dissipation of energy causes the decrease of the streamwise fluctuating component, u, one can get the energy length scale:

$$Lu = -(u'^2)^{3/2} / \left(U \frac{\partial u'^2}{\partial x} \right) \ , \tag{4}$$

where $u' = \sqrt{\overline{u^2}}$ is the streamwise velocity standard deviation. Knowing that for the isotropic turbulence the rate of dissipation of turbulence kinetic energy can be written as

$$\varepsilon = -\frac{3}{2} U \frac{\partial u'^2}{\partial x} \tag{5}$$

(Dyban *et al.* [8], see also Ames and Moffat [9]), one can determine the scale Lu as follows:

$$Lu = \frac{3}{2} \frac{u'^3}{\varepsilon} \ . \tag{6}$$

To distinguish the length scale Lu, Eq. (4) or Eq. (6) from the integral scale L (2), we will call it the *dissipation length scale*.

The measure of the average dimension of the small eddies involved in fluid motion is the time microscale of turbulence

$$\tau_E = \left(-\frac{1}{2} \frac{\partial^2 \mathbf{R}}{\partial t} \bigg|_{t=0} \right)^{-1/2} = \left(\frac{1}{2 \left\langle u_i^2 \right\rangle} \left\langle \left(\frac{\partial u_i}{\partial t} \right)^2 \right\rangle \right)^{-1/2} , \tag{7}$$

which can be called the Eulerian dissipation time scale [7]. Finally, between the time microscale, τ_E, and the length microscale, λ, the simple relation is received

$$\lambda = U \tau_E \, . \tag{8}$$

The scale λ is called the Taylor microscale (otherwise, Hinze names this one the dissipation scale [7]).

The characteristic turbulence scales are also associated with the particular ranges of the turbulence energy spectrum, $E(k)$. Special attention can be paid to the form of $E(k)$ in the inertial subrange, for which the Kolmogorov spectrum law is fulfilled:

$$E(k) = C_k \, \varepsilon^{2/3} \, k^{-5/3} \, , \tag{9}$$

where k is the longitudinal wave number and C_k is the Kolmogorov constant (for a one-dimensional spectrum). The universal equilibrium range of the energy spectrum, in which the function $E(k)$ is under the influence of only two values, i.e., dissipation, ε, and the kinematic viscosity of the fluid, ν, can be described by the following scale:

$$\eta = \frac{1}{k_\eta} = \left(\frac{\nu^3}{\varepsilon} \right)^{1/4} \, . \tag{10}$$

This is the measure of the smallest eddies in the flow and it is called the Kolmogorov length scale (k_η is the wave number corresponding to this scale).

In the dissipative range of the energy spectrum one can distinguish one more characteristic scale, $l_d = 1/k_d$, which determines the size of the eddies corresponding to the maximum of the dissipation spectrum

$$\varepsilon = \int_0^\infty D(k) dk = 2\nu \int_0^\infty k^2 E(k) dk \, . \tag{11}$$

The maximum of the function $D(k)$ is defined by the wave number k_d within a range of $0.15 \leq k_\eta \leq 0.5$ (Townsend [10]) or $0.09 \leq k_\eta \leq 0.5$ in the case of very large Reynolds numbers (Hinze [7], after Kraichnan [11]). The maximum of

the $E(k)$ function, determined by the wave number $k_e = 1/l_e$, lies in a relatively narrow range occupied by the eddies containing most of the energy and corresponding to the length scale similar to the integral scale.

The turbulent integral length scale, L, can also be estimated based on the total turbulent kinetic energy, $K_T = \frac{1}{2}\overline{u_i' u_i'}$, and the dissipation rate, ε, [12]:

$$L = \frac{K_T^{3/2}}{\varepsilon} \ . \tag{12}$$

Otherwise, at enough high Reynolds numbers, the local viscous dissipation rate, ε, of the local average turbulent kinetic energy scales with K and a local correlation length scale L (see, for example Batchelor [13], Townsend [10], Valente and Vasilicous [14]):

$$\varepsilon \sim \frac{K_T^{3/2}}{L} \ . \tag{13}$$

Referring to Taylor's theory [15], for decaying homogeneous isotropic turbulence or to analyses of wind-tunnel simulations of such turbulence (e.g., Batchelor and Townsend [16], Comte-Bellot and Corrsin [17]) we can write the integral scale in the form

$$L = C_\varepsilon \frac{u'^3}{\varepsilon} \ , \tag{14}$$

where C_ε is a constant independent on time, space and Reynolds number when the Reynolds number is large enough. The data compilation of Sreenivasan [18], suggested that C_ε does become constant at Taylor Reynolds number (based on the microscale λ), $\mathrm{Re}_\lambda = u\lambda/\nu$, larger than about 50 for wind-tunnel turbulence generated by various biplane square-mesh grids, but it seems to differ from the results of other authors' investigations, e.g., Lumley [19], Valente and Vasilicous [14].

3 Isotropy of turbulence

In general, the turbulence intensity is defined as the ratio of standard deviation to the mean flow velocity, U. If the velocity field is described by the coordinate system x_i, where x_1 is an axis oriented in the direction of the mean flow velocity ($U = U_1,\ U_2 = U_3 = 0$), a ratio

$$Tu = Tu_1 = \frac{\sqrt{\overline{u_1^2}}}{U} = \frac{u_1'}{U} \tag{15}$$

defines the longitudinal turbulence intensity, while

$$Tu_2 = \frac{u_2'}{U} \quad \text{and} \quad Tu_3 = \frac{u_3'}{U} \tag{16}$$

are the components of the transverse intensity. In case of isotropic turbulence which characteristics do not depend on the spatial orientation of the coordinate system, we have

$$\overline{u_1^2} = \overline{u_2^2} = \overline{u_3^2}\,. \tag{17}$$

The isotropic turbulence has a probability density function (PDF) close do Gaussian [20]. One of the methods to assess the isotropy of turbulence is to determine the skewness factor in the flow velocity distribution [21,22]

$$S(u) = \frac{\overline{u^3}}{\sqrt{\overline{u^2}^3}}\,. \tag{18}$$

The turbulence is isotropic, if the skewness is zero and hence, a PDF of the variable u has normal distribution.

A similar way to assess the turbulence isotropy is the kurtosis (flatness factor) that is also a descriptor of the shape of the probability distribution of the velocity fluctuations. The measure of kurtosis is a fourth central moment of mean velocity divided by the standard deviation to the fourth power

$$K(u) = \frac{\overline{u^4}}{\sqrt{\overline{u^2}^4}}\,. \tag{19}$$

When $K(u) = 3$, the probability distribution is normal. When $K(u) < 3$ or $K(u) > 3$ probability distribution is called platykurtic (flat shape) or leptokurtic (focused shape), respectively.

In the opinion of Batchelor the distribution can be considered as normal for the value of $K(u) = 2.86$ [13], Jimenez gives the value of $K(u) = 2.85$ [23]. The grid distance, x, from which turbulence may be considered to be nearly isotropic, is $x/M > 40$ (Gad-el-Hak and Corrsin [24]), where M is the mesh size of a grid.

One of the methods to gain isotropic turbulence is to achieve high Reynolds number that is difficult with the use of 'conventional' (or static) grids. In the opinion of Gad-el-Hak and Corrsin [24], turbulence isotropy improvement can be attained by the active (or dynamic) grids that are equipped with controllable nozzles. This technique has been used for example by Makita [25] and improved by Mydlarski and Warhaft [26,27], where a Taylor Reynolds number

of the order of 700 was achieved [27]. An attempt to gain isotropic turbulence at low Reynolds number was recently made by Birouk, Sarh and Gokalp [28]. For this purpose an experimental apparatus, a turbulence chamber 'box', was used to generate an isotropic turbulent flow field in the center of the chamber, even though the Reynolds number achieved in this experiment is considered to be small, $\mathrm{Re}_\lambda < 100$.

4 Experimental equipment and procedure

The investigation was carried out in the subsonic wind tunnel of low level of turbulence, $Tu \approx 0.1\%$ and with velocity range up to 100 m/s. The sketch of the test section and the details of the leading edge is shown in Fig. 1. The measurement chamber with octagonal cross-section has the following dimensions (width, height, length) 600 x 460 x 1500 mm. The boundary layer was studied on the upper surface of the flat plate of the length 700 mm. The enhanced level of turbulence was generated by five different wicker metal grids (with square meshes) of the following dimensions:

1) $d = 0.3$ mm, $M = 1$ mm,
2) $d = 0.6$ mm, $M = 3$ mm,
3) $d = 1.6$ mm, $M = 4$ mm,
4) $d = 3.0$ mm, $M = 10$ mm,
5) $d = 3.0$ mm, $M = 30$ mm

(named appropriately G1, G2, G3, G4, and G5), where d is a diameter of the grid rod and M is a grid mesh size. Grids were placed at different distances upstream of the plate leading edge: $L_s = 450$, 410, 370, and 330 mm. Also five different incoming velocities were used: $U = 10$, 15, 20 m/s (for G1 and G2), $U = 6$, 10, 15, and 20 m/s (for G3), $U = 6$ and 10 m/s (for G4) and $U = 4$ and 6 m/s (for G5).

The coordinate system for the turbulence intensity and scale measurements is fixed to the grid with x-coordinate parallel to the mean velocity of the flow. The coordinate system for boundary layer measurements is fixed to the leading edge of the plate. The plate leading edge location is equal to L_s downstream of the grid, as mentioned above.

The velocity and turbulence measurements were carried out by means of the StreamLine thermoanemometry system (Dantec) with the software Stream-Ware 3.41.20 and the hot-wire probe 55P15 of Dantec suitable for measurements in boundary layer.

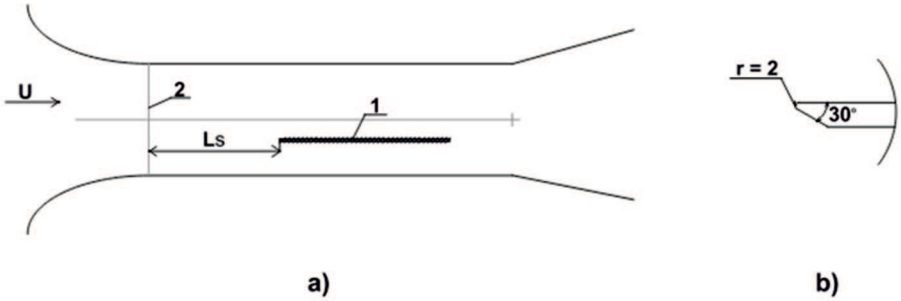

Figure 1: Test section of wind tunnel: a) 1 – flat plate, 2 – grid at the distance L_s from the leading edge; b) shape of the leading edge.

First measurements of the turbulence decay behind all grids were carried out, and then the velocity profiles in the boundary layer on a flat plate in different distances from the leading edge. To avoid separation at the leading edge the incidence angle of the plate $i = -1.63°$ was set (boundary layer with favourable pressure gradient). Therefore a small velocity gradient along the plate was measured. A value of the acceleration parameter

$$a = \frac{\nu}{U^2}\frac{dU}{dx}\,, \tag{20}$$

where U is the mean flow velocity and ν is the kinematic viscosity, was approximately 2.7×10^{-7}. The effect of favourable pressure gradient on boundary layer receptivity one can find, e.g., in [29].

The boundary layer profiles were determined by the measurement of velocity in about forty points across the boundary layer. The sampling frequency of the velocity signal was 6 kHz and 40000 samples were taken, i.e., for about 6.67 s. Before every measurements series the calibration of system was carried out.

5 Investigation results

5.1 Turbulence isotropy tests

Many of the formulas listed in this article refer to the isotropic turbulence, so it was important to assess what kind of turbulence we have to do with in the experiment. First of all, isotropy of turbulence of the flow behind the grids was investigated. To assess the value of the distance x/M (M – mesh size), from which the turbulence is considered to be isotropic, skewness factor along the test section of the tunnel in case without turbulence generator (without grid) was measured.

Values of skewness for mean flow velocities $U = 6, 10$, and 15 m/s are displayed in Fig. 2. Here the distance x is normalized by the measurement chamber length $L_c = 1500$ mm. The turbulence intensity, Tu, did not exceed in this case the value of 0.13 %. As we can see, skewness factor $S(u)$, for all three flow velocities ranges approximately from 0 to 0.06 throughout the measured region. It was assumed that turbulence is isotropic if the skewness does not exceed the value of 0.06.

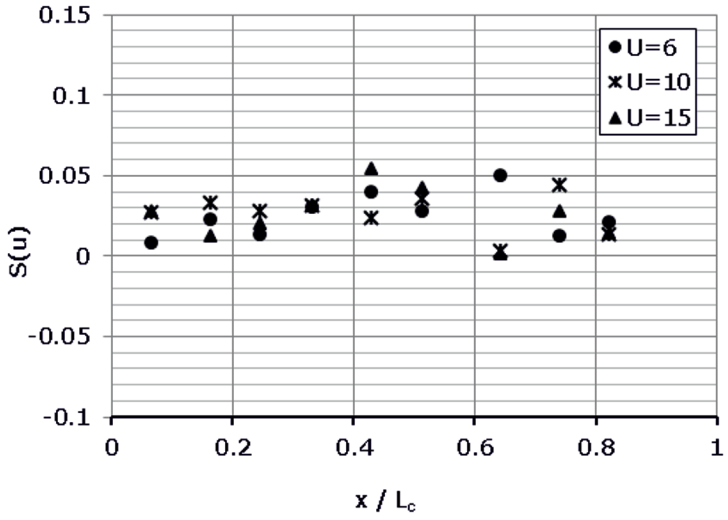

Figure 2: Skewness along the measurement chamber in case of no turbulence generator, for mean flow velocities $U = 6$, 10, and 15 m/s.

Figures 3 and 4 present the skewness factor, $S(u)$, and kurtosis, $K(u)$, for grids G3 and G5, depending on x/M. Fig. 3 shows the results for velocities $U = 6, 10, 15$, and 20 m/s. Directly behind the grid, for $x = 90$ mm, i.e., $x/M = 22.5$, skewness is different from zero (Fig. 3a), but does not exceed 0.13 at the highest point. Then tends to zero, which indicates that the probability density function of the variable u' approaches the Gaussian distribution. Over the plate (from $x/M = 112.5$ which corresponds to the point of the leading edge) we observe the skewness not exceeding 0.06. Kurtosis, which is presented in Fig. 3b, is a bit greater than 3, but does not exceed the value of 3.06. Over the plate $K(u)$ ranges from 2.86 to 3.04, which means that turbulence can be considered as nearly isotropic.

Directly behind the grid G5 (Fig. 4) the flow is strongly anisotropic. At the distance of $x/M = 1.5$ from the grid, $S(u) = -0.09$, $K(u) = 2.59$ for $U = 4$ m/s and $S(u) = -0.27$, K$(u) = 2.67$ for $U = 6$ m/s. The skewness is negative because

of the bar wakes velocity fluctuations that are smaller than the average velocity flow fluctuations. Generally, the sign of $S(u)$ indicates the direction of the largest velocity fluctuations while the magnitude of $S(u)$ shows the degree of asymmetry in the distribution of the fluctuations [30]. From the leading edge ($x/M = 15$) we observe general increase in values of skewness and kurtosis factors. For $x/M = 33$ skewness is still high, $S(u) = 0.16$, and $K(u)$ is smaller than 2.85, which means the PDF of the velocity fluctuations is still not Gaussian, hence the turbulence is anisotropic. The values of $S(u)$ and $K(u)$ for other grids and velocities one can find, for example, in [31]. The summary of turbulence isotropy investigation for grids G1–G5 near the plate edge ($L_S = 450$ mm) has been presented in Tab. 1.

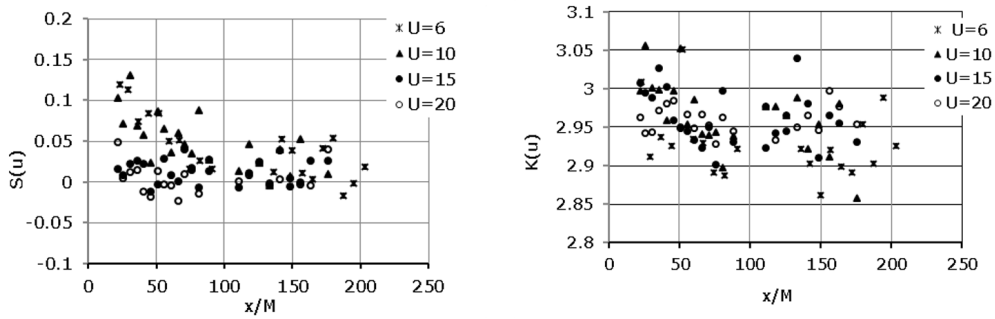

(a) (b)

Figure 3: Skewness (a) and kurtosis (b) for the grid G3 and flow velocities $U = 6$, 10, 15, and 20 m/s.

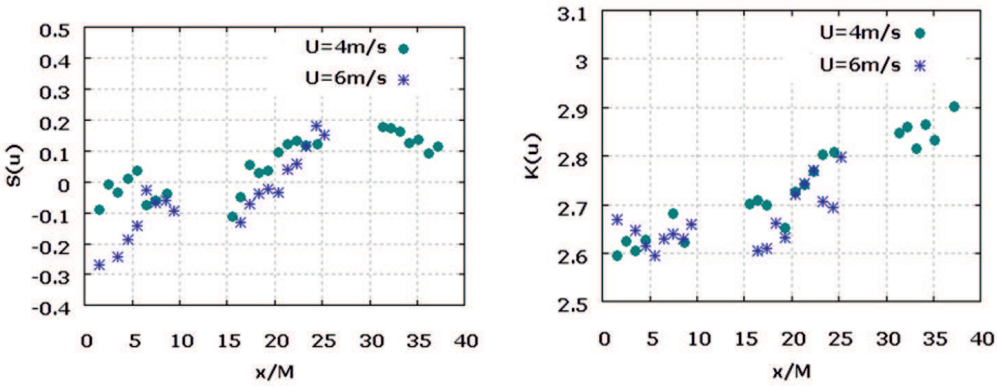

(a) (b)

Figure 4: Skewness (a) and kurtosis (b) for the grid G5 and flow velocities $U = 4$ and 6 m/s.

Table 1: Values of skewness and kurtosis for grids G1–G5 near the plate leading edge (L_S = 450 mm).

Grid	U [m/s]	$S(u)$	$K(u)$	x/M ($x = L_s = 450$ mm)
G1 (M=1, d=0.3)	10–20	-0.01 – (-0.005)	2.97 – 3.03	450
G2 (M=3, d=0.6)	15–20	0.02 – 0.04	2.87 – 2.89	150
G3 (M=4, d=1.6)	6–20	-0.01 – 0.05	2.92 – 2.98	112.5
G4 (M=10, d=3)	6–10	0.04 – 0.07	2.87 – 2.89	45
G5 (M=30, d=3)	4–6	-0.13 – (-0.11)	2.60 – 2.70	15

Summarizing, turbulence of the flow behind grids was considered to be nearly isotropic from the distance $x/M = 70$. The values of x/M, $S(u)$, and $K(u)$ for grids G1–G4 and for all flow velocities used in the experiment are displayed in Tab. 2. (For G1 the distance is $x/M = 90$, but it was the first point measured behind the grid, i.e., $x = 90$ mm).

Table 2: Values of the distance x/M for grids G1–G4, from which the turbulence is considered to be isotropic.

Grid	U [m/s]	$S(u)$	$K(u)$	x/M
G1	10	0.050	3.00	90
	15	0.057	3.00	90
	20	-0.033	3.03	90
G2	10	0.036	2.90	60
	15	0.035	2.90	60
	20	0.057	2.88	70
G3	6	0.049	2.93	60
	10	0.059	2.94	66
	15	0.028	2.94	56
	20	-0.0234	2.97	66
G4	6	0.047	2.91	61
	10	0.060	2.94	67

5.2 Scales of turbulence

To investigate the turbulence scale dependence on the transition inception, which was the main goal of the experiment, determining the length scale behind the grid was first needed. To determine the dissipation scale, Lu, and Kolmogorov scale, η, knowledge of the rate of turbulence kinetic energy dissipation, ε, was required. Therefore the turbulence energy spectrum, $E(k)$, was measured.

An example of the spectrum over the boundary layer, for the selected grid G3 and mean velocity $U = 10$ m/s is plotted in Fig. 5. The grid distance in this case was $L_s = 450$ mm and the thermoanemometric probe distance was 230 mm downstream from the leading edge. The straight line ($k^{-5/3}$) represents the inertial subrange of the turbulence spectrum. For the above conditions the subrange of wave numbers are 204 l/m $\leq k \leq$ 620 l/m which gives the values of the range of length scale 1.6 mm $\leq l \leq$ 4.9 mm.

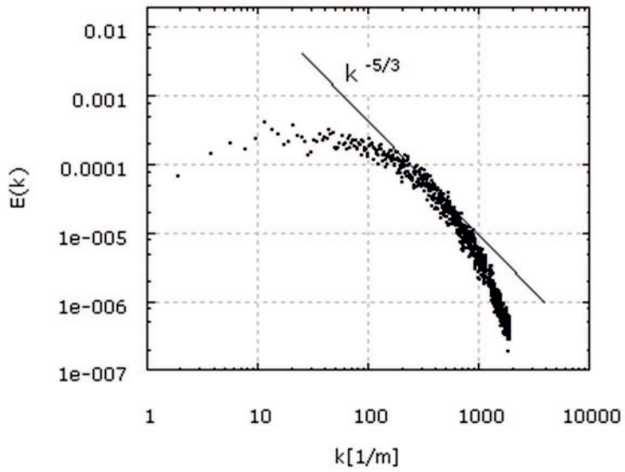

Figure 5: Turbulence energy spectrum, $E(k)$, for turbulence generated by the grid G3, flow velocity $U = 10$ m/s, over the plate at the distance of 230 mm from the leading edge.

The time correlation coefficient (3) and the parabola whose positive root determines the time microscale, τ_E, are plotted in Fig. 6. In this case, according to the formula (8), turbulence time microscale $\tau_E = 0.28$ ms, which gives the Taylor microscale $\lambda = 2.8$ mm, so it is included in the inertial subrange of the turbulence spectrum (Fig. 5). As recommended by Fouladi *et al.* [30] the time microscales should be derived from the intersection of a parabola, fitted to the first three to five points of the correlation curve. In this case it was not possible, because the sampling frequency was 6 kHz, so only two first points were taken.

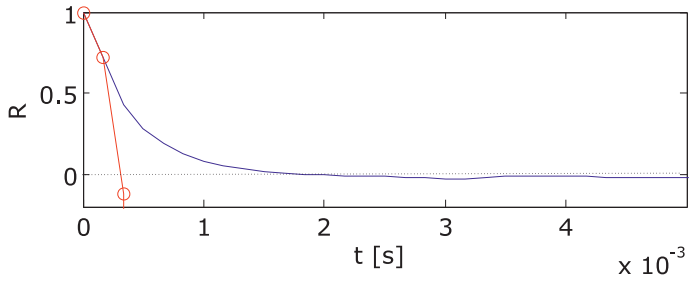

Figure 6: The time correlation coefficient, R, versus time, t, (solid line) and the parabola fitted curve (solid line with circles), which determines the time scale, τ_E, for G3, $U = 10$ m/s, at the distance of 230 mm downstream from the leading edge.

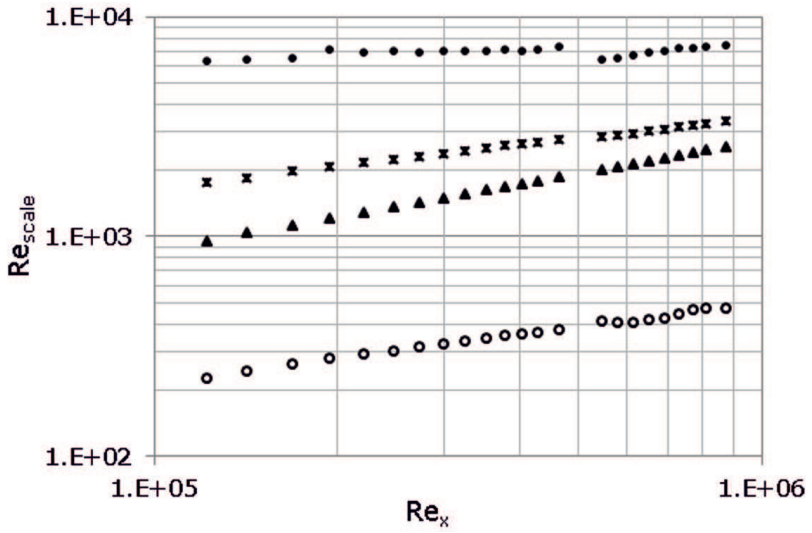

Figure 7: Reynolds number based on the scale of turbulence behind the grid G2, for mean flow velocity $U = 20$ m/s: • – integral scale L Eq. (2), **x** – dissipation scale Lu Eq. (6), ▲ – Taylor microscale λ Eq. (8), ○ – Kolmogorov scale η Eq. (10).

In Fig. 7 different kinds of turbulence length scales are presented, for the selected grid G3, the velocity of the flow $U = 10$ m/s and the grid distance $L_s = 450$ mm from the leading edge of the plate. To make the values normalized, Reynolds numbers were used. The abscissa presents Reynolds number based on distance x downstream from the leading edge, $\mathrm{Re}_x = Ux/\nu$, and the ordinate – Reynolds number based on corresponding length scale – $\mathrm{Re}_{scale} = U_{scale}/\nu$ here scale represents the characteristic linear dimension. The integral scale L, associated with the

largest eddies in the flow has of course the largest dimension; then we have a bit smaller dissipation scale, Lu, Taylor microscale, λ, and finally the Kolmogorov scale, η, as the measure of the smallest eddies. To compare turbulence scales for different grids but for the same flow velocity $U = 10$ m/s, Reynolds numbers based on all four mentioned length scales have been plotted (Fig. 8). Generally, the larger grid dimensions M and d, the larger scales values L and Lu. The exception refers to the Taylor microscale, which is almost the same for all four grids G1–G4 and Kolmogorov scale, which has the biggest value in case of the grid with the smallest parameters.

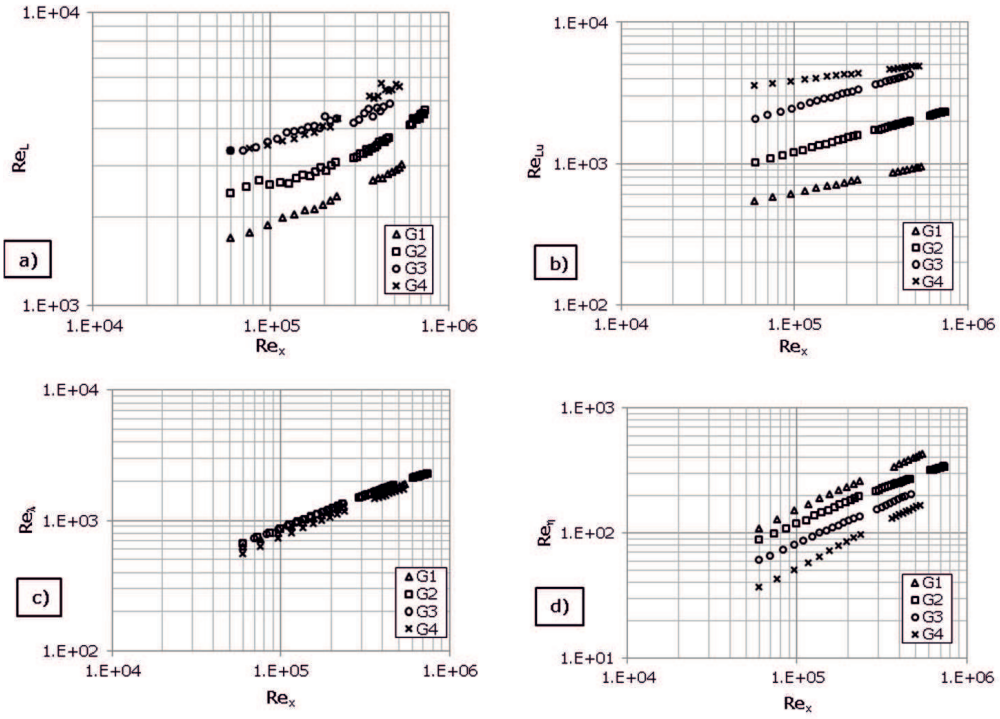

Figure 8: Length scale Reynolds number for mean velocity $U = 10$ m/s and different grids G1, G2 , G3 , and G4: a) integral scale L, b) dissipation scale Lu, c) Taylor microscale λ, d) Kolmogorov scale η.

To compare length scales for one grid (G3) but different flow velocities ($U =$ 6, 10, 15, and 20 m/s), Fig. 9 is displayed. Generally, the larger value of the flow velocity, the larger value of the integral scale Reynolds number, Re_L, and dissipation scale Reynolds number, Re_{Lu}. For the Taylor microscale λ and the Kolmogorov scale η, Reynolds numbers lie almost on the same curve, but one

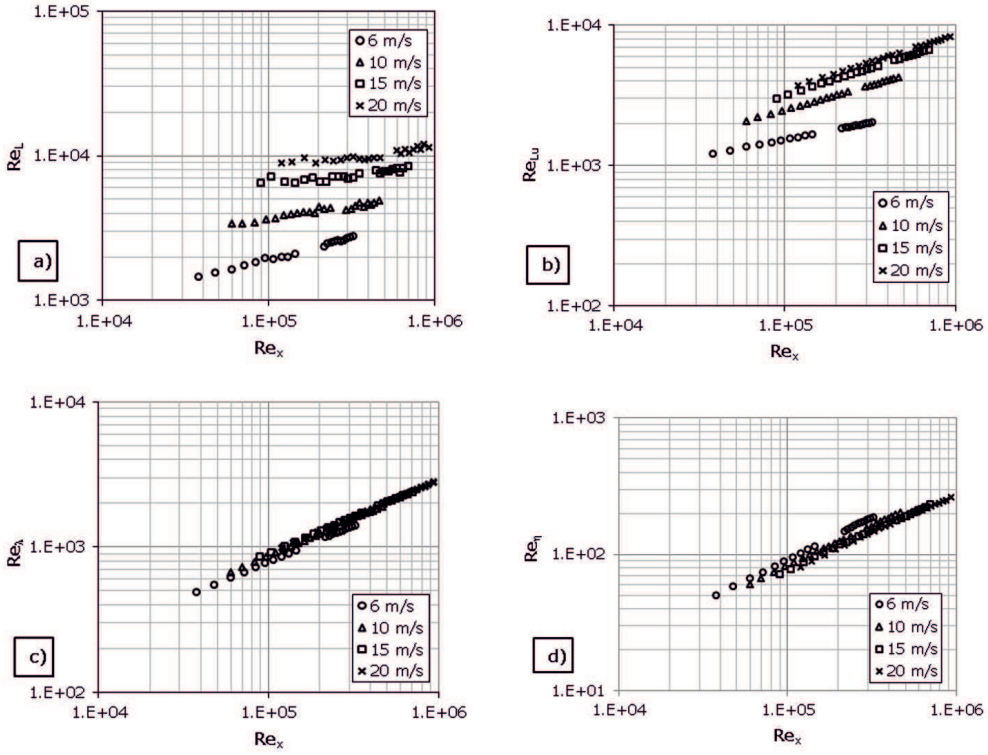

Figure 9: Length scale Reynolds numbers for the grid G3 and different flow velocities $U = 6$, 10, 15, and 20 m/s: a) integral scale L, b) dissipation scale Lu, c) Taylor microscale λ, d) Kolmogorov scale η.

can notice the opposite trend for Re_η, which has the biggest value in case of the smallest velocity, 6 m/s. Looking at both Figs. 8 and 9 it may be stated that reducing the wall shear stress causes a slower evolving of large eddies and faster evolving of small eddies.

5.3 Correlation of the transition

Having determined the length scale of turbulence and the momentum thickness Reynolds number of the onset of transition, Re_t^{**}, one can find the correlation function. To create the correlation, the dissipation scale, Lu, values at the leading edge of the plate were used. The turbulence intensity at the leading edge for grids G1–G4 was from $Tu = 0.4\%$ to 3.4% and for grid G5 exceeded the value of 4%, moreover the turbulence was not isotropic at the measured points in case of grid

G5. All numerical values of distance L_s, turbulence intensity, Tu, and scale, Lu, at the plate leading edge (x_0) for all grids and flow velocities are presented in Tab. 3.

The results of present investigations seem to confirm the results of Jonas [4], but only if we make correlation for all grids together (Fig. 10; the dashed line represents the formula (1)). But when we look at every grid separately, the results seem not to be that obvious. Because of the result points dispersion the investigations need to be verified, but according to the present ones the momentum thickness Reynolds number, Re_t^{**}, increases (which means the transition appears later) when Lu increases, for grids G2 and G3. If the values of the Reynolds number Re_t^{**} start to become smaller than 200 (as we have for the grid G5), the transition appears earlier when the values of the length scale Lu are larger.

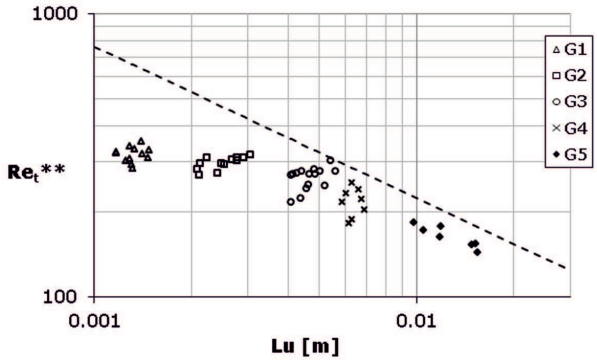

Figure 10: Momentum thickness Reynolds number at the onset of transition as a function of turbulence scale, Lu, for different grids, flow velocities and grid distances; the dashed line represents the formula (1).

The turbulence scale at the formula (1) can be changed in the dimensionless formula using one of the grid parameters

$$\mathrm{Re}_t^{**} = k \left(\frac{Lu}{d} \right)^m \quad , \tag{21}$$

where we have chosen a rod diameter, d. Figure 11 shows the results for Re_t^{**} as a function of Lu/d, for grids of different dimensions. For G1–G4 coefficient of the formula is $k = 158$, while exponent $m = 0.455$, and for G5 $k = 305$, $m = -0.436$. When the value of Lu/d increases, the transition appears later for the grids G1–G4 and earlier for the grid G5, but we keep in mind that in the last case the turbulence is anisotropic. Besides, the values for the grid G4 seem to belong to both correlations.

Table 3: Values of distance L_s, turbulence intensity and scale at plate leading edge for grids G1–G5 and all flow velocities.

Grid	M [mm]	d [mm]	L_S [mm]	U [m/s]	$Tu(x_0)$ [%]	$Lu(x_0)$ [mm]
G1	1	0.3	450	10	0.41	1.29
				15	0.41	1.40
				20	0.39	1.41
			410	10	0.42	1.34
				15	0.42	1.48
				20	0.40	1.46
			370	10	0.47	1.17
				15	0.46	1.29
				20	0.44	1.26
			310	10	0.51	1.17
				15	0.52	1.31
				20	0.49	1.32
G2	3	0.6	450	10	0.81	3.06
				15	0.74	2.77
				20	0.66	2.24
			410	10	0.86	2.91
				15	0.79	2.67
				20	0.70	2.13
			370	10	0.92	2.77
				15	0.84	2.49
				20	0.76	2.08
			310	10	0.98	2.53
				15	0.92	2.42
				20	0.82	2.11
G3	4	1.6	450	6	1.47	4.41
				10	1.58	5.43
				15	1.52	5.60
				20	1.41	5.20
			410	6	1.60	4.26
				10	1.68	5.12
				15	1.63	5.01
				20	1.49	4.55
			370	6	1.74	4.14
				10	1.82	4.82
				15	1.77	4.86
				20	1.62	4.37
			310	6	1.89	4.09
				10	1.99	4.66
				15	1.92	4.62
				20	1.76	4.07

Tab. 3 continued

Grid	M [mm]	d [mm]	L_S [mm]	U [m/s]	Tu(x_0) [%]	Lu(x_0) [mm]
G4	10	3	450	6	2.55	6.30
				10	2.56	6.75
			410	6	2.65	6.62
				10	2.69	6.90
			370	6	3.04	6.03
				10	3.09	6.28
			310	6	3.36	5.87
				10	3.40	6.17
G5	30	3	450	4	4.13	9.81
				6	4.13	11.93
			410	4	4.44	10.53
				6	4.19	14.57
			370	4	4.63	11.82
				6	4.39	15.27
			310	4	4.98	14.88
				6	4.66	15.47

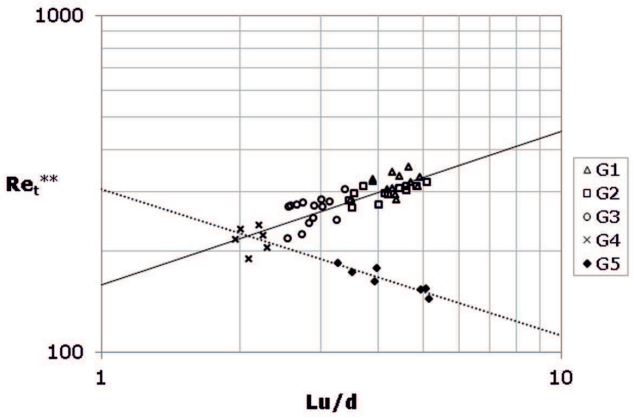

Figure 11: Momentum thickness Reynolds number at the onset of transition as a function of Lu/d.

6 Concluding remarks

To investigate the phenomena of turbulent flow, five wicker grids with square meshes and different parameters (diameter of the grid rod range 0.3 mm$\leq d \leq$3 mm and the grid mesh size range 1 mm $\leq M \leq$ 30 mm were used to generate turbulence. The turbulence intensity at the leading edge of the plate was from

$Tu = 0.4\%$ to 4%. Several longitudinal scales of turbulence were determined, i.e., integral scale L, dissipation scale, Lu, Taylor microscale, λ, and Kolmogorov scale, η. To assess the isotropy of turbulence, the skewness and kurtosis factors of the flow velocity distribution were determined. For grids G1–G4, where respectively ($d = 0.3$ mm, $M = 1$ mm, $Tu = 0.4\%$)–($d = 3$ mm, $M = 10$ mm, $Tu = 3.4$ %), the isotropic turbulence throughout the measured chamber was obtained. For the grid G5 ($d = 3$ mm, $M = 30$ mm, $Tu = 4$ %) the skewness and kurtosis factors indicated that the turbulence was anisotropic.

The influence of the turbulence intensity and turbulence scale on the laminar–turbulent bypass transition location on a flat plate was investigated. In this case the dissipation scale, Lu, at the leading edge was taken into account. For this purpose, the momentum thickness Reynolds number, $\mathrm{Re}_t{}^{**}$, at which transition onset appears, was calculated. Present investigations seem to confirm the results indicating that the boundary layer laminar-turbulent inception moves downstream with the decreasing of turbulence scale, but only if we make correlation for all grids together. But when we take into account a single grid, especially G2 ($d = 0.6$ mm, $M = 3$ mm) and G3 ($d = 1.6$ mm, $M = 4$ mm), the results are not so obvious or even seem to be quite opposite. However, in present investigation turbulence intensity was also the variable (the same as turbulence scale) and not constant as it was for example in paper of Jonas *et al.* [4].

Dividing the turbulence scale by the grid rod diameter, dimensionless formula was proposed (21). Finally, we can say that the investigation indicates that the decreasing of turbulence scale (divided by the grid wire diameter, d) provides an earlier inception, i.e., the lower momentum thickness Reynolds number for grids G1–G4, but a later inception for grid G5, which generates anisotropic flow turbulence in the whole test section.

It seems reasonable to take into account also other turbulence length scales, because till now, only the dissipation length scale Lu was used to make the correlation of the transition. Besides parameter d was the only one that was used to propose the dimensionless formula of the transition correlation. Probably the thickness, momentum or displacement thickness of the boundary layer could be taken into account. Moreover the result points' scatter is quite big and the present investigations still need some revision and improvement.

Received 3 Oct. 2016 (revised form 3 April 2018)

References

[1] Mayle R.E.: *The Role of laminar – turbulent transition in gas turbine engines*. J. Turbomach. **113**(1991), 4, 509–537.

[2] Hall D.J., Gibbings J.C.: *Influence of stream turbulence and pressure gradient on boundary – layer transition*. J. Mech. Eng. Sci. **14**(1972), 2, 134–146.

[3] Abu-Ghannam B.J., Shaw R: *Natural transition of boundary layers – The effects of turbulence, pressuer gradient, and flow history*. J. Mech. Eng. Sci. **22**(1980), 5, 213–228.

[4] Jonas P., Mazur O., Uruba V.: *On the receptivity of the by – pass transition to the length scale of the outer stream turbulence*. Eur. J. Mech. B-Fluids **19**(2000), 5, 707–722.

[5] Epik E.J.: *Bypass laminar-turbulent transition in a thermal boundary layer*. Inz. Fiz. Zh. (J. Eng. Phys. Thermophys.) **74**(2001), 4, 105–110 (in Russian).

[6] Barret M.J., Hollingsworth D.K.: *On the calculation of length scales for turbulent heat transfer correlation*. ASME J. Heat Transfer **123**(2001), 5, 878–883.

[7] Hinze I.O.: *Turbulence*. McGraw Hill Book Company, 1975. [

[8] Dyban E.P., Epik E.J., Suprun T.T., Juszyna L.E.: *Simulation of flows with controlled turbulence levels and turbulence scales*. Promyshlennaya teplotechnika (Ind. Heat Eng.) **18**(1996), 2, 60–73 (in Russian).

[9] Ames F.E., Moffat R.J.: *Heat Transfer with High Intensity, Large Scale Turbulence: The Flat Plate Turbulent Boundary Layer and the Cylindrical Stagnation Point*. Report No. HMT-44, Department of Mechanical Engineering, Stanford University, Stanford 1990.

[10] Townsend A.A.: *The Structure of Turbulent Shear Flow*. Cambridge University Press, 1956.

[11] Kraichnan R.H.: Isotropic turbulence and inertial-range structure. Phys Fluids **9**(1966), 9, 1728.

[12] Xiao H., Wang J., Jenny P.: *Dynamic evaluation of mesh resolution and its application in hybrid LES/RANS methods*. Flow Turbul. Combust. **93**(2014), 1, 141–170.

[13] Batchelor G.K.: *The theory of homogeneous turbulence*. Cambridge University Press, 1953.

[14] Valente P.C., Vassilicos J.C.: *The decay of turbulence generated by a class of multiscale grids*. J. Fluid Mech. **687**(2011), 300–340.

[15] Taylor G.I.: *Statistical theory of turbulence*. Proc. R. Soc. A **151**(1935), 873, 421–444.

[16] Batchelor G.K., Townsend A.A.: *Decay of isotropic turbulence in the initial period*. Proc. R. Soc. A **193**(1948), 1035, 539–558.

[17] Comte-Bellot G., Corrsin S.: *The use of a contraction to improve the isotropy of grid-generated turbulence*. J. Fluid. Mech. **25**(1966), 4, 657–682.

[18] Sreenivasan K.R.: *On the scaling of the turbulence energy dissipation rate*. Phys. Fluids **27**(1984), 5, 1048.

[19] Lumley W.K.: *Some comments on turbulence*. Phys. Fluids A **4**(1992), 2, 203–211.

[20] Van Atta C.W., Chen W.Y.: *Measurements of spectral energy transfer in grid turbulence*. J. Fluid Mech. **38**(1969), 4, 743–763.

[21] Mohamed M.S, LaRue J.C.: *The decay power law in grid-generated turbulence*. J. Fluid Mech. **219**(1990), 195–214.

[22] Ting D.S.K.: *Some Basics of Engineering Flow Turbulence* (revised Edn.). Naomi Ting's Book, Windsor 2013.

[23] Jimenez J.: *Turbulent velocity fluctuations need to be Gaussian*. J. Fluid Mech. **376**(1998), 139–147.

[24] Gad-el-Hak M., Corrsin S.: *Measurements of the nearly isotropic turbulence behind a uniform jet grid*. J. Fluid Mech. **62**(1973), 1, 115–143.

[25] Makita H.: *Realization of a large-scale turbulence field in a small wind tunnel*. Fluid Dyn. Res. **8**(1991), 1-4, 53–64.

[26] Mydlarski L., Warhaft Z.: *On the onset of high-Reynolds-number grid-generated wind tunnel turbulence*. J. Fluid. Mech. **320**(1996), 331–368.

[27] Mydlarski L., Warhaft Z.: *Passive scalar statistics in high-Peclet-number grid turbulence*. J. Fluid. Mech. **358**(1998), 135–175.

[28] Birouk M., Sarh B., Gokalp I.: *An attempt to realize experimental isotropic turbulence at low Reynolds number*. Flow Turbul. Combust. **70**(2003), 1-4, 325–348.

[29] Johnson M.W., Pinarbasi A.: *The effect of pressure gradient on boundary layer receptivity*. Flow Turb. Combust. **93**(2014), 1, 1–24.

[30] Fouladi F., Henshaw P., Ting D.S.K.: *Turbulent flow over a flat plate downstream of a finite height perforated plate*. ASME J. Fluid Eng. **137**(2015), 2, 021203-1.

[31] Grzelak J., Wierciński Z.: *The decay power law in turbulence generated by grids*. Trans. Inst. Fluid-Flow Mach. **130**(2015), 93–107.